PAPER

Check for updates

Biomass-derived nitrogen-doped hierarchically porous carbon networks as efficient absorbents for phenol removal from wastewater over a wide pH range

Wenyi Du,[a] Junting Sun,[a] Yongxi Zan,[a] Zhengping Zhang,[ab] Jing Ji,[ab] Meiling Dou*[ab] and Feng Wang ⓘ *[ab]

Developing cost-effective porous carbon adsorbents with large adsorption capacity and superior recyclability over a wide pH range is critical for the efficient removal of toxic phenol from industrial wastewater. Herein, we demonstrate a facile and effective strategy for synthesis of a nitrogen-doped hierarchically porous carbon (NHPC) network derived from cattle bone as a highly efficient adsorbent for the removal of phenol from wastewater. The as-prepared NHPC possessed a high specific surface area (2687 m^2 g^{-1}), a unique three-dimensional (3D) hierarchical porous structure and high content of nitrogen doping (2.31 at%). As a result, NHPC exhibited a remarkable adsorption performance towards phenol with a significantly large adsorption capacity of 431 mg g^{-1} (3.56-fold that of the commercial adsorbent (Norit CGP)), a high adsorption rate of 4.57 g mg^{-1} h^{-1} (17-fold that of Norit CGP) and an outstanding recyclability with 98% of the initial adsorption capacity maintained after 5 cycles (75% for Norit CGP). More importantly, the NHPC held almost the identical maximum adsorption capacity over a wide pH range of 2–9, showing a good applicability in the removal of phenol from a variety of wastewaters. Thermodynamic and kinetics analyses indicated that the adsorption process was spontaneous and exothermic, which fitted well the Langmuir isotherm model and pseudo-second-order model. This biomass-based porous carbon with well-defined hierarchical porosity can be applied as a promising adsorbent for efficient removal of phenol from wastewater.

1. Introduction

Phenols that are commonly discharged from the wastewater of petroleum refineries and steel foundries, pose a great threat to the health and safety of both human beings and animals due to their high toxicity and carcinogenicity even at low concentrations.[1] Many technologies including membrane separation,[2] photocatalytic degradation,[3] and adsorption[4] have been developed for phenol removal from wastewater. Among them, the adsorption technique is regarded as a competitive and effective approach due to its simplicity and high efficiency.[5,6] However, the poor recyclability of the adsorbents in the adsorption technique limits its performance, resulting in a high-cost and tedious procedure for the removal of phenols from wastewater. Consequently, great efforts have been devoted to the development of highly efficient, recyclable and low-cost adsorbents for the removal of phenols.

Over the past decades, porous carbon materials have been widely used as alternative adsorbents due to their relatively high adsorption performances originating from the large specific surface area, high porosity, and abundant surface functionalities.[7–11] Unfortunately, the adsorption performance including adsorption capacity, adsorption rate and recyclability of most previously reported porous carbons are still far from satisfactory on the removal of phenol because of their torturous porous channels and numerous inaccessible micropores that limit the diffusion and adsorption of the phenol molecules in the pores.[12,13] In addition, their adsorption performances are also highly susceptible to the pH value of the target phenol-containing wastewaters,[14,15] which is hampering the large-scale application of porous carbon adsorbents for industrial wastewaters with various pH values. To address these issues, it is essential for porous carbon absorbents to have a large specific surface area and an interconnected hierarchically micro–meso–macro-porous structure, in which the micropores can increase the amount of accessible adsorption sites, and the open meso/macropores can promote the mass transport of phenols in

[a]State Key Laboratory of Chemical Resource Engineering, Beijing Key Laboratory of Electrochemical Process and Technology for Materials, Beijing University of Chemical Technology, Beijing 100029, P. R. China. E-mail: wangf@mail.buct.edu.cn; douml@mail.buct.edu.cn; Fax: +86-10-64451996; Tel: +86-10-64451996

[b]Beijing Advanced Innovation Center for Soft Matter Science and Engineering, Beijing University of Chemical Technology, Beijing 100029, P. R. China

wastewaters. Besides, the phenol absorption is determined not only by the "π–π dispersion interaction" between the carbon basal plane and the phenol aromatic ring, but also by the "donor–acceptor effect" between the surface functional groups and the phenol molecules.[16,17] In this regard, surface modification of porous carbon by nitrogen-containing functional groups (e.g., –NH$_2$, pyrrolic N, quaternary N) plays an important role in the enhancement of adsorption performance of porous carbon absorbents due to the formation of donor–acceptor complex.[18] Also, these nitrogen-containing functional groups on the porous carbon surfaces can be expected to alleviate the effect of solution pH on the phenol adsorption,[16] leading to an enhanced adsorption flexibility over a wide pH range. Based on these design principles, it is evident that the nitrogen-doped hierarchically porous carbons with large specific surface area are promising as efficient adsorbents for the removal of phenols from wastewaters.

Recently, biomass materials (e.g., cattle bone,[19] chitosan[20] and silkworm cocoon[21]) have emerged as a new platform for synthesizing the functional porous carbon materials due to their unique structural characteristics, abundant source and wide available features. As one kind of biomass wastes, animal bone consisting of organic collagens with ordered inorganic composites is an ideal precursor for synthesizing nitrogen-doped porous carbon.[22,23] The organic collagens can be converted to carbon with rich nitrogen doping, and the high porosity and three-dimensional (3D) ordered nano-architecture of animal bone can be partially preserved to afford large specific surface area of resultant porous carbon due to the template effect of ordered inorganic composites via a facile carbonization approach. In the present study, we developed a facile and effective strategy for synthesis of nitrogen-doped 3D hierarchical porous carbon (NHPC) networks as an efficient adsorbent for the removal of phenol from wastewater via the carbonization and KOH activation of cattle bone (Scheme 1). NHPC with nitrogen doping possessed a large specific surface area of 2687 m^2 g^{-1} and a well-defined 3D hierarchically porous structure. As used as an adsorbent for phenol removal, the resultant NHPC exhibited a remarkable adsorption performance over a wide pH range with a large adsorption capacity, a high adsorption rate and an outstanding recyclability, far superior to that of the commercial porous carbon adsorbent NORIT CGP SUPER (Norit CGP, activated carbon).
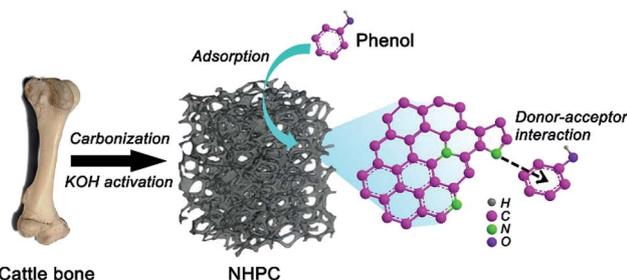
Scheme 1 Schematic illustration of synthetic process of NHPC for efficient removal of phenol.

2. Materials and methods

2.1. Adsorbents and reagents

The dried cattle bone powder was purchased from market in Beijing. High-purity Ar gas (99.99%) was bought from Beijing AP BAIF Gases Industry Co., Ltd. Potassium hydroxide (KOH) and hydrogen nitrate (HNO$_3$) were analytical grade produced by Sinopharm. The Norit CGP was purchased from Norit company (Beijing). Ultrapure water (Millipore, 18.2 MΩ cm) was used throughout the preparation. All the materials were used as received without further purification.

2.2. Synthesis of NHPC

The NHPC was synthesized by pyrolyzing the dried cattle bone powder based on the previous work.[19] Briefly, the dried cattle bone powder was firstly pre-carbonized at 400 °C for 3 h in an Ar atmosphere and then mixed with KOH at an optimized mass ratio of 1.67. Subsequently, the mixture was transferred into the tubular furnace and carbonized at 800 °C for 1 h in an Ar atmosphere. After carbonization with KOH-activation, the product was washed with 2 mol L^{-1} HNO$_3$ followed by rinsing with ultrapure water until the filtrate was neutral, and then dried at 120 °C for 24 h under vacuum to obtain NHPC.

2.3. Characterizations

Scanning electron microscopy (SEM) was performed with a field emission scanning electron analyzer (FE-JSM-6701F, JEOL, Japan) operating at an accelerating voltage of 10 kV. Transmission electron microscope (TEM) was carried out on a (JSM-2100 instrument (JOEL, Japan)) operating at 300 kV. N$_2$ adsorption–desorption measurements were performed with an automatic Quantachrome II analyzer to evaluate the total specific surface area (based on the Brunauer–Emmett–Teller (BET) model) and pore-size distribution (based on the density functional theory (DFT) model) of the absorbents. Fourier transform infrared spectroscopy (FT-IR) (Nicolet 6700, USA) and X-ray photoelectron spectroscopy (XPS) (ESCALAB-250, Thermo Fisher Scientific, USA) analyses were used to determine the element composition and surface chemical state of the absorbents. The concentration of phenol in aqueous solution was determined using ultraviolet spectrophotometer (UV-2450, Japan) at a wavelength of 269.5 nm.

2.4. Adsorption of phenol

Batch adsorption of phenol experiments were conducted with a reciprocal shaker bath (Chunlan Co., Ltd.). Prior to adsorption, 1000 mg L^{-1} phenol solution was firstly prepared by diluting the stock solution using deionized water. The pH value of phenol solution was adjusted by 0.01 mol L^{-1} HCl or 0.01 mol L^{-1} NaOH. Afterwards, 0.01 g of as-prepared NHPC was added in a vial with 10 mL of phenol solution (the phenol concentration of 125 ppm) and rotated at 130 rpm for 4 h at 303 K. After adsorption equilibrium, the solution was filtered, and the filtrate was collected to analyze the phenol concentration. For comparison, the adsorption of phenol with Norit CGP

was also conducted under the identical conditions. The equilibrium adsorption capacity of phenol (q_e, mg g^{-1}) was calculated according to the following equation:[8]

$$q_e = (C_0 - C_e)/m \times V \quad (1)$$

where, V (L) is the volume of the phenol solution, C_0 (mg L^{-1}) and C_e (mg L^{-1}) are the initial and equilibrium concentration of phenol, respectively, and m (g) is the mass of NHPC used.

Langmuir (eqn (2)) and Freundlich models (eqn (3)) were applied to fit the adsorption data to describe the adsorption equilibrium of NHPC and Norit CGP.[23]

$$q_e = q_m \times b \times C_e/(1 + b \times C_e) \quad (2)$$

$$q_e = K_F \times C_e^{1/n} \quad (3)$$

where, C_e (mg L^{-1}) is the equilibrium concentration of phenol, q_e (mg g^{-1}) is the amount of phenol adsorbed, q_m (mg g^{-1}) is the saturate adsorption capacity of phenol, b (L mg^{-1}) is the Langmuir isotherm coefficient, K_F (mg g^{-1}) and n are the Freundlich constants.

2.5. Adsorption kinetics and thermodynamic

Pseudo-first-order (eqn (4)) and pseudo-second-order (eqn (5)) models were used to investigate the adsorption kinetics of phenol removal.[23]

$$\log(q_e - q_t) = \log q_e - kt/2.303 \quad (4)$$

$$t/q_t = 1/(kq_e^2) + t/q_e \quad (5)$$

where, q_e (mg g^{-1}) is the adsorption capacity, q_t (mg g^{-1}) is the adsorption capacity at time (h), and k (g mg^{-1} h^{-1}) is the rate constant of the adsorption process.

Thermodynamic analysis of phenol adsorption was also investigated according to eqn (6) and (7) to calculate the thermodynamic parameters including Gibbs free energy change (ΔG, kJ mol^{-1}), enthalpy change (ΔH, kJ mol^{-1}) and entropy change (ΔS, J mol^{-1} K^{-1}).[24]

$$\Delta G = -RT \ln b \quad (6)$$

$$\ln b = \Delta S/R - \Delta H/(RT) \quad (7)$$

where, R (8.314 kJ mol^{-1} K^{-1}) is the ideal gas constant, T (K) is the adsorption temperature, and b (L mol^{-1}) is the Langmuir constant.

2.6. Regeneration experiment

After the equilibrium adsorption in phenol solution, the adsorbents were washed with ethanol in the reciprocal shaker bath for several times to remove the adsorbed phenol and then dried under vacuum at 303 K for 24 h for regeneration. Afterwards, the regenerated adsorbents were reused for the adsorption of phenol in the consecutive adsorption–desorption cycles.

3. Results and discussion

3.1. Physicochemical characterization

The as-prepared NHPC was first characterized by SEM, TEM, and N$_2$ adsorption–desorption measurements to investigate the microstructure and porosity properties. The representative SEM and TEM images (Fig. 1) combined with N$_2$ adsorption–desorption analysis (Fig. 2a) shows that the NHPC exhibits a 3D hierarchically porous structure with abundant micropores (1–2 nm, micropore surface area of 1072 m^2 g^{-1}) along with interconnected open mesopores (2–6 nm) and macropores (50–200 nm). The total specific surface area and pore volume of NHPC are determined as 2687 m^2 g^{-1} and 2.1 cm^3 g^{-1}, respectively, significantly higher than those of Norit CGP (1929 m^2 g^{-1} and 1.37 cm^3 g^{-1}) and most reported biomass-based porous carbon phenol adsorbents (Table 1). The larger specific surface area along with the abundant micropores are favorable for the enhancement of adsorption capacity by providing sufficient adsorption sites, while the interconnected open meso/macropores are believed to promote the mass transfer of phenol, leading to an improved adsorption rate of NHPC.

Besides the porosity properties, the configuration of surface functional groups is considered another important factor that determines the adsorption behavior of the porous carbon adsorbents for phenol removal. The FT-IR spectrum of NHPC in Fig. 2b exhibits the stretching vibrations of O–H & N–H (3439 cm^{-1}), C–H (2921 cm^{-1} and 2852 cm^{-1}), C=O & C=N (1618 cm^{-1}), and C–O (1222 cm^{-1}). The O–H, C=O and C–O groups are probably contributed from the etching effect of KOH on the porous carbon networks during activation process. The existence of nitrogen-containing functional groups (i.e., N–H and C=N) are derived from the carbonization of the organic collagens in cattle bone. The surface contents of O and N elements are determined as 12.37 at% and 2.31 at% by XPS measurement, respectively. The high-resolution N 1s spectra of NHPC before and after the adsorption of phenols (Fig. 2c and d) can be deconvoluted into four peaks located at approximately 399.5 eV, 400.5 eV, 401.2 eV, and 402.2 eV, showing the presence of pyridinic N, pyrrolic N, graphitic N and oxidized N, respectively.

To explore the effect of these surface functional groups on the adsorption of phenol, the surface physicochemical
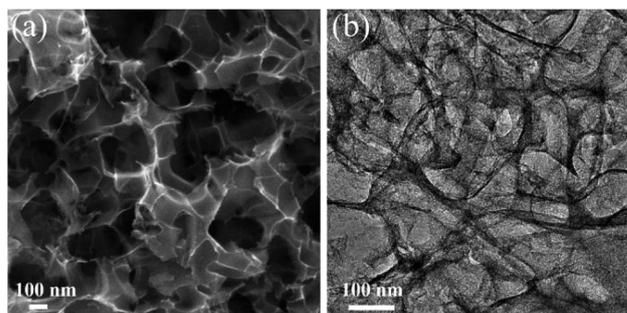

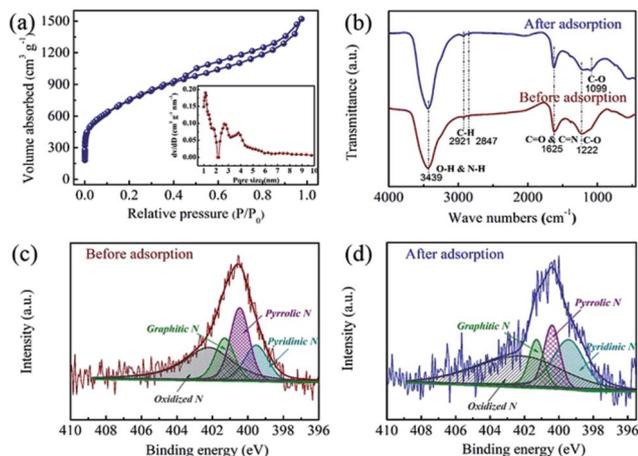Fig. 1 Representative (a) SEM and (b) TEM images of NHPC.

Fig. 2 (a) N_2 adsorption–desorption isotherm (inset: pore size distribution) of NHPC, (b) FT-IR spectra of NHPC before and after phenol adsorption, and high-resolution XPS N 1s spectra of NHPC (c) before and (d) after phenol adsorption.

properties of NHPC after adsorption were also characterized. FT-IR spectrum (Fig. 2b) of NHPC presents a distinct peak located at approximately 1098.6 cm^{-1} after the adsorption of phenol, which is associated with the vibration of phenolic type C–O bond,[25] indicating the adsorption of phenol on NHPC. The XPS analysis of the N 1s spectrum of NHPC after adsorption in Fig. 2d shows an obvious decrease of pyrrolic N (from 27.5 to 17.1 at%) accompanied with an increase of pyridinic N (from 17.1 to 26.9 at%) and a slight changes of graphitic N and oxidized N in comparison with those of NHPC before adsorption (Fig. 2c). The variation of N configuration before and after the phenol adsorption implies that the surface nitrogen groups are interacted with phenol molecule, and the pyrrolic N may contribute to the formation of donor–acceptor complex with phenol molecule by donating the lone pair electrons,[17] promoting the adsorption of phenol on NHPC.

3.2. Adsorption performance

3.2.1. Effect of the solution pH.
To evaluate the adsorption performance of NHPC for the removal of phenol from wastewater, effects of the solution pH, initial phenol concentration and contact time on the adsorption capacity were investigated and compared with Norit CGP. The effect of the solution pH on the adsorption capacity of NHPC (Fig. 3a) shows that its maximum adsorption capacity is approximately 110 mg g^{-1} as the pH ranging from 2 to 9, significantly higher than that of Norit CGP (60 mg g^{-1}). This feature can be attributed to the fact that the NHPC possesses a large specific surface area and well-defined 3D hierarchical porous structure to host the adsorbed phenol molecule, and the existence of surface carbonyl and pyrrolic N groups may attract the phenol molecule onto the surface through the "π–π dispersion interaction" and "donor–acceptor effect".[17] It is worth noting that the adsorption capacity of NHPC remains almost the same over the pH range of 2–9,
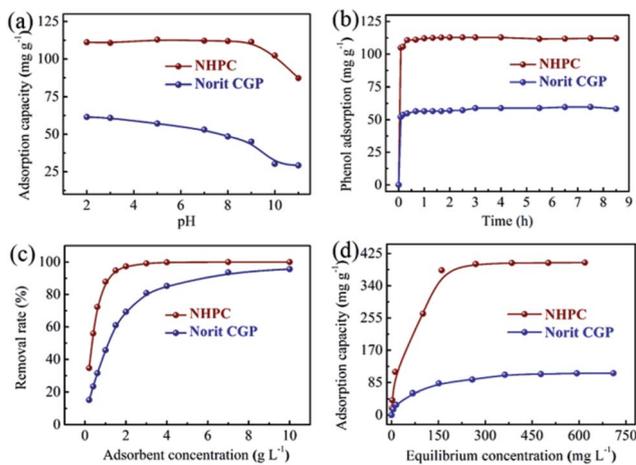

Fig. 3 Effect of (a) the solution pH, (b) initial phenol concentrations, and (c) contact time on the adsorption capacities of NHPC and Norit CGP. (d) Adsorption isotherms of NHPC and Norit CGP at 303 K.

Table 1 Summary of the phenol adsorption performance of absorbents reported in the literature

Adsorbents	BET (m^2 g^{-1})	Q (mg g^{-1})	pH	K (g mg^{-1} h^{-1})	Recyclability	Ref.
Coffee residue derived carbon	520	88.31	3	—	—	12
Seeds derived carbon	206	90	4–8.5	13.56	—	13
Tea waste derived carbon	1066	142.9	4–8	0.144	—	25
Eggshells derived carbon	113	192	5.2	—	—	26
Soybean straw derived carbon	2271	208	—	—	—	27
Corn grain derived carbon	2135	256	3–6	0.96	—	28
activated sericite	59.6	1.502	5.0	1.03	38%	29
MOFs	2174	330	—	7.4×10^{-3}	28%	30
Au NPs	—	6.54	4	0.62	90%	31
Rattan sawdust derived activated carbon	—	149.25	—	—	—	32
Granular activated carbon	—	165.80	—	—	—	33
Commercial activated carbon	—	49.72	—	—	—	34
Sugarcane bagasse fly ash	—	23.832	—	—	—	35
Activated carbon-commercial grade	—	30.2187	—	—	—	35
Activated carbon-laboratory grade	—	24.6458	—	—	—	35
Commercial Norit CGP	1929	121	3	0.27	75%	This work
NHPC	2687	431	2–9	4.57	98%	This work

much different from Norit CGP with obviously decreased adsorption capacity as the pH value increased, indicating that the NHPC is more robust against the pH value and favorable for phenol removal from wastewaters with various pH values. The stable adsorption capacity over the pH range of 2–9 for NHPC may be attributed to the abundant surface oxygenated and nitrided groups which are capable of alleviating the effect of solution pH on phenol adsorption.[16] However, it should be mentioned that the adsorption capacities of both NHPC and Norit CGP suddenly decrease as the solution pH exceeds 9. At such pH value, the dissociation of phenol occurrs since the pK_a of phenol is 9.98.[17] The resultant phenolate anions (negative charge) repels the negative charged surface of NHPC (pH > pH_{pzc} = 3.4) due to the electrostatic interaction between the phenolate anions and NHPC, leading to a decrease of adsorption capacity. In addition, the decreased adsorption capacity is also attributed to the stronger interaction between water and phenolate anions that is more soluble in aqueous solution.[16]

3.2.2. **Effect of contact time and initial phenol concentration.** Apart from the flexibility of solution pH, rapid adsorption with a short time is also extremely important for the efficient removal of phenol for industrial applications. Fig. 3b shows the variations of the adsorption capacities of both NHPC and Norit CGP in the function of contact time at the initial phenol concentration of 125 ppm. It is apparent that the adsorption of phenol on NHPC can quickly reach the adsorption equilibrium with a shorter contact time (1 h) than that of Norit CGP (4 h). Also, approximately 83.9% and 41.5% of phenol can be removed by NHPC and Norit CGP within only 5 minutes, respectively, suggesting a faster adsorption rate of phenol on NHPC than Norit CGP. The relatively high adsorption rate of NHPC is mainly attributed to the high-flow mass transport of phenol from solution to the adsorption sites on NHPC due to its well-defined interconnected open meso/macropores. Additionally, the effect of initial phenol concentrations on the adsorption capacities of NHPC and Norit CGP was also investigated (Fig. 3c). The adsorption capacities of NHPC and Norit CGP increase as increasing the adsorbent concentration (from 0.2 to 10 g L^{-1}), and keep constant as the initial phenol concentration exceeds 3 g L^{-1} and 10 g L^{-1} for NHPC and Norit CGP, respectively. The maximum phenol removal rate is determined as almost 98% for NHPC, rather higher than that of Norit CGP (75%), further confirming the superior adsorption performance of NHPC.

3.3. Adsorption isotherms

Fig. 3d shows the adsorption isotherm of NHPC recorded at 303 K at various initial phenol concentrations (20–819 mg L^{-1}). The NHPC exhibits a significantly larger adsorption capacity (18–401 mg g^{-1}) than that of Norit CGP (15–109 mg g^{-1}) even at low initial phenol concentrations, which is attributed to its hierarchically porous structure with large specific surface area that provides sufficient accessible adsorption sites. The Langmuir isotherm model (eqn (2)) and Freundlich isotherm model (eqn (3)) have been applied to describe the adsorption behavior of phenol on NHPC (Table 2). The adsorption isotherm data can be better defined by the Langmuir model with a high correlation coefficient value ($R^2 > 0.99$), indicating a monolayer adsorption behavior. The maximum adsorption capacity of NHPC is calculated as high as 431 mg g^{-1}, which is 3.56-fold the corresponding value of Norit CGP (121 mg g^{-1}) and much higher than those of most reported porous carbon adsorbents (Table 1). The significantly higher adsorption capacity of NHPC compared with Norit CGP is attributed to the larger specific surface area and pore volume of NHPC (1.4 and 1.7-fold that of Norit CGP, respectively), which can increase absorption sites and facilitate mass transfer for phenol. In addition, the surface N-containing groups of NHPC also contribute to the enhancement of adsorption performance due to the formation of donor–acceptor complex.

3.4. Adsorption kinetics and thermodynamics

The adsorption kinetics of NHPC were investigated based on the pseudo-first-order (eqn (4)) and pseudo-second-order models (eqn (5)). The calculated correlation coefficient values (R^2) in Table 3 indicates that the adsorption process is well described by the pseudo-second-order model with a much larger R^2 (1.00) than that of pseudo-first-order model (0.82), which is similar as that of the biosorption of Cd(II)[36] and Pb(II).[37] Based on this model, the rate constant (k) of NHPC is calculated to be 4.57 g mg^{-1} h^{-1}, almost 17-fold that of Norit CGP (0.27 g mg^{-1} h^{-1}), further confirming that the NHPC possesses a high adsorption rate for the removal of phenol.

To further investigate the adsorption process of NHPC, the thermodynamics parameters including ΔG, ΔH and ΔS were calculated according to eqn (6) and (7). As shown in Table 4, the negative ΔG value at each temperature (303 K, 313 K and 323 K) indicates that the phenol adsorption on NHPC is a spontaneous

Table 2 Parameters of Langmuir and Freundlich models for the adsorption of phenol on NHPC and Norit CGP

Adsorbent	Temp. (K)	Langmuir model			Freundlich model		
		q_m (mg g^{-1})	b (L mg^{-1})	R^2	K_F (mg g^{-1})	$1/n$	R^2
NHPC	303	431	0.028	0.992	129	0.186	0.54
	313	383	0.025	0.994	115	0.184	0.64
	323	340	0.025	0.999	131	0.141	0.78
Norit CGP	303	121	0.015	0.998	32.5	0.191	0.90
	313	140	0.0071	0.991	18.5	0.285	0.96
	323	148	0.0091	0.990	25.5	0.250	0.91

Table 3 Parameters of the pseudo-first-order and pseudo-second-order models for the adsorption of phenol on NHPC

| Sample	Temp. (K)	Pseudo first order		Pseudo second order	
		k_1 (h^{-1})	R^2	k_2 (g mg^{-1} h^{-1})	R^2
NHPC	303	1.50	0.818	4.57	0.99996
Norit CGP	303	0.57	0.844	0.27	0.99998

Table 4 Thermodynamic parameters for the adsorption of phenol on NHPC

Sample	ΔH^o (kJ mol^{-1})	ΔS^o (J K^{-1} mol^{-1})	ΔG^o (kJ mol^{-1})		
			30 °C	40 °C	50 °C
NHPC	−3.98	52.1	−19.8	−20.2	−20.9

process. Furthermore, the adsorption capacity decreases with increasing the adsorption temperature, suggesting that the phenol adsorption on NHPC is an exothermic process, which is also verified by the negative value of ΔH (−3.98 kJ mol^{-1}). This feature is different from the endothermic adsorption of Pb(II) ions from waste water.[37]

3.5. Recyclability of NHPC

The recyclability is an important factor that determines the application potential of the adsorbent for the removal of phenol. We further evaluated the recyclability of NHPC and Norit CGP towards phenol removal by the regeneration experiment at room temperature with regeneration of NHPC and Norit CGP in ethanol aqueous solution. As expected, the NHPC adsorbent (Fig. 4) exhibits a superior recyclability with approximately 98% of its initial adsorption capacity after 5 cycles, whereas the Norit CGP retains only 75% of its initial adsorption
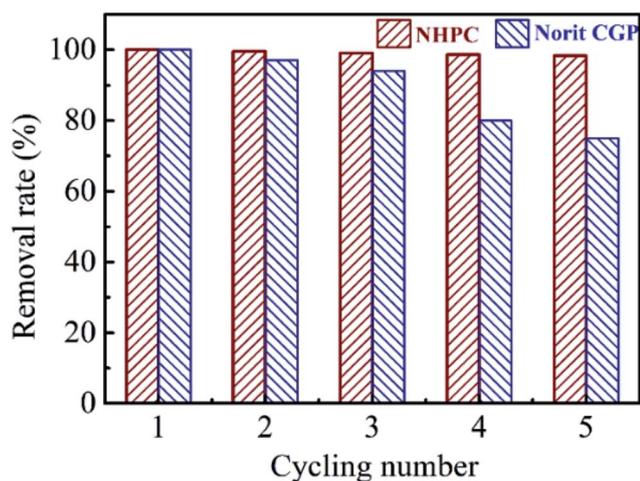
capacity. The remarkably superior recyclability of NHPC compared with Norit CGP is mainly attributed to its 3D hierarchically porous structure with interconnected open meso/macropores networks that promotes not only adsorption of phenol into NHPC but also desorption of phenol from NHPC. Therefore, the NHPC possesses a remarkably large adsorption capacity over a wide pH range, high adsorption rate, and superior recyclability of phenol solution, making it a promising adsorbent for potential large-scale application for the removal of phenol.

4.   Conclusions

In summary, we have developed a facile and effective strategy for synthesis of nitrogen-doped hierarchically porous carbon (NHPC) networks as highly efficient adsorbent for the removal of phenol from wastewater *via* the carbonization and KOH activation of cattle bone. The well-defined 3D hierarchical porous structure with a large specific surface area of 2687 m^2 g^{-1} not only facilitates the quick transfer of the phenol molecules in the pore, but also provides sufficient accessible adsorption sites for the adsorption of phenols. Moreover, the doped nitrogen atoms in NHPC further promote the adsorption of phenol *via* the formation of donor–acceptor complex with phenol molecule by donating the lone pair electrons. Consequently, the NHPC exhibits a remarkable adsorption performance with a significantly larger adsorption capacity, a higher adsorption rate and a superior recyclability in comparison with Norit CGP. Furthermore, the NHPC is robust against the pH variation of phenol solution, exhibiting almost the identical maximum adsorption capacity over a wide pH range of 2–9. Thermodynamic and kinetic analyses indicate that the adsorption of phenol on NHPC is well defined by the Langmuir isotherm model and pseudo-second-order model, and the adsorption process is spontaneous and exothermic. This work develops a low-cost and effective methodology for the design and synthesis of hierarchically porous carbon adsorbents with superior adsorption performance for removal of phenol.

Conflicts of interest

There are no conflicts to declare.

Acknowledgements

References

1 S. Yuan, J. Gu, Y. Zheng, W. Jiang, B. Liang and S. O. Pehkonen, *J. Mater. Chem. A*, 2000, **3**, 4620.
2 M. Hemmati, N. Nazari, A. Hemmati and S. Shirazian, *J. Ind. Eng. Chem.*, 2015, **21**, 1410.
3 J. E. Casillas, F. Tzompantzi, S. G. Castellanos, G. Mendoza-Damián, R. Pérez-Hernández, A. López-Gaona and A. Barrera, *Appl. Catal., B*, 2017, **208**, 161.

Fig. 4 The removal rate of NHPC and Norit CGP for phenol at different adsorption–desorption cycles.

4 W. Tang, H. Huang, Y. Gao, X. Liu, X. Yang, H. Ni and J. Zhang, *Mater. Des.*, 2015, **88**, 1191.

5 M. H. Dehghani, M. Mostofi, M. Alimohammadi, G. McKay, K. Yetilmezsoy, A. B. Albadarin, B. Heibati, M. AlGhouti, N. M. Mubarak and J. N. Sahu, *J. Ind. Eng. Chem.*, 2016, **35**, 63.

6 N. K. Mondal, R. Bhaumik, B. Das, P. Roy, J. K. Datta, S. Bhattacharyya and S. Bhattacharjee, *Appl. Water Sci.*, 2014, **5**, 271.

7 O. G. Apul and T. Karanfil, *Water Res.*, 2015, **68**, 34.

8 B. Chang, W. Shi, D. Guan, Y. Wang, B. Zhou and X. Dong, *Mater. Lett.*, 2014, **126**, 13.

9 M. Wisniewski, A. P. Terzyk, P. A. Gauden, K. Kaneko and Y. Hattori, *J. Colloid Interface Sci.*, 2012, **381**, 36.

10 W. Bunmahotama, W.-N. Hung and T.-F. Lin, *Water Res.*, 2015, **85**, 521.

11 G. Yang, L. Tang, G. Zeng, Y. Cai, J. Tang, Y. Pang, Y. Zhou, Y. Liu, J. Wang, S. Zhang and W. Xiong, *Chem. Eng. J.*, 2015, **259**, 854.

12 K. Lamia and B. Farida, *J. Chem. Eng. Data*, 2010, **55**, 4677.

13 L. A. Rodrigues, M. L. C. P. da Silva, M. O. Alvarez-Mendes, A. d. R. Coutinho and G. P. Thim, *Chem. Eng. J.*, 2011, **174**, 49.

14 J. Feng, K. Qiao, L. Pei, J. Lv and S. Xie, *Ecol. Eng.*, 2015, **84**, 209.

15 K. Mohanty, D. Das and M. N. Biswas, *Chem. Eng. J.*, 2005, **115**, 121.

16 G. Yang, H. Chen, H. Qin and Y. Feng, *Appl. Surf. Sci.*, 2014, **293**, 299.

17 A. D. browski, P. Podkościelny, Z. Hubicki and M. Barczak, *Chemosphere*, 2005, **58**, 1049.

18 E. Lorenc-Grabowska, G. Gryglewicz and M. A. Diez, *Fuel*, 2013, **114**, 235.

19 M. Dou, D. He, W. Shao, H. Liu, F. Wang and L. Dai, *Chem.– Eur. J.*, 2016, **22**, 2896.

20 U. Soni, J. Bajpai, S. K. Singh and A. K. Bajpai, *J. Water. Process Eng.*, 2017, **16**, 56.

21 J. Sun, Z. Zhang, J. Ji, M. Dou and F. Wang, *Appl. Surf. Sci.*, 2017, **405**, 372.

22 H. Liu, Y. Cao, F. Wang and Y. Huang, *ACS Appl. Mater. Interfaces*, 2014, **6**, 819.

23 S. Wei, D. Li, Z. Huang, Y. Huang and F. Wang, *Bioresour. Technol.*, 2013, **134**, 407.

24 H. N. Tran, S.-J. You, A. Hosseini-Bandegharaei and H.-P. Chao, *Water Res.*, 2017, **120**, 88.

25 A. Gundogdu, C. Duran, H. B. Senturk, M. Soylak, D. Ozdes, H. Serencam and M. Imamoglu, *J. Chem. Eng. Data*, 2012, **57**, 2733.

26 L. Giraldoa and J. C. Moreno-Piraján, *J. Anal. Appl. Pyrolysis*, 2014, **106**, 41.

27 Q. Miao, Y. Tang, J. Xu, X. Liu, L. Xiao and Q. Chen, *J. Taiwan Inst. Chem. Eng.*, 2013, **44**, 458.

28 K.-H. Park, M. S. Balathanigaimani, W.-G. Shim, J.-W. Lee and H. Moon, *Microporous Mesoporous Mater.*, 2010, **127**, 1.

29 Lalhmunsiama, D. Tiwari and S.-M. Lee, *Chem. Eng. J.*, 2016, **283**, 1414.

30 B. N. Bhadra, I. Ahmed and S. H. Jhung, *Fuel*, 2016, **174**, 43.

31 J. Pal, M. K. Deb and D. K. Deshmukh, *Res. Chem. Intermed.*, 2014, **41**, 8363.

32 B. H. Hameed and A. A. Rahman, *J. Hazard. Mater.*, 2008, **160**, 576.

33 A. Kumar, S. Kumar, S. Kumar and D. V. Gupta, *J. Hazard. Mater.*, 2007, **147**, 155.

34 B. Ozkaya, *J. Hazard. Mater.*, 2006, **129**, 158.

35 V. C. Srivastava, M. M. Swamy, I. D. Mall, B. Prasad and I. M. Mishra, *Colloids Surf., A*, 2006, **272**, 89.

36 H. J. He, Z. H. Xiang, X. J. Chen, H. Chen, H. Huang, M. Wen and C. P. Yang, *Int. J. Environ. Sci. Technol.*, 2017, DOI: 10.1007/s13762-017-1507-8.

37 Y. Cheng, C. Yang, H. He, G. Zeng, K. Zhao and Z. Yan, *J. Environ. Eng.*, 2016, **142**, C4015001.